Research Square

Preprints are preliminary reports that have not undergone peer review.
They should not be considered conclusive, used to inform clinical practice,
or referenced by the media as validated information.

Unveiling the Role of Melatonin in Coronary Heart Disease: Identification and Experimental Validation of Novel Biomarkers

Yongchao Peng
First Affiliated Hospital of Nanchang University
Xuemin Zhou
Jiangxi Provincial People's Hospital, The First Affiliated Hospital of Nanchang Medical College)
Yaowu Xie
Jiangxi Provincial People's Hospital, The First Affiliated Hospital of Nanchang Medical College)
Li Huang
Jiangxi Provincial People's Hospital, The First Affiliated Hospital of Nanchang Medical College)
Xuanlan Chen
Jiangxi Provincial People's Hospital, The First Affiliated Hospital of Nanchang Medical College)
Zhifeng Zhang
zhangzhifengzz@163.com

Jiangxi Provincial People's Hospital, The First Affiliated Hospital of Nanchang Medical College)

Article

Keywords: coronary heart disease, biomarkers, bioinformatics analysis, therapeutic targets

Posted Date: April 21st, 2026

DOI: https://doi.org/10.21203/rs.3.rs-8816168/v1

License: This work is licensed under a Creative Commons Attribution 4.0 International License.
Read Full License

Additional Declarations: No competing interests reported.

Abstract

Melatonin (ME) affects multiple systems in coronary heart disease (CHD), including lipid/glucose metabolism, blood pressure, and sleep-wake regulation, while also promoting coronary thrombosis through unknown mechanisms. This study uses bioinformatics to identify ME-related biomarkers for CHD diagnosis and treatment. The GSE179789 and GSE113079 datasets were obtained from a public database. Biomarkers were selected via differential analysis and expression validation. Gene set enrichment analysis (GSEA) was performed, and regulatory as well as drug-biomarker networks were constructed. Biomarker expression was further validated in clinical samples using RT-qPCR. MAP2K2 and PGD were identified as reliable CHD biomarkers, showing significant up-regulation in CHD samples across both datasets. GSEA indicated their involvement in multiple pathways, including ribosome, prion diseases, and Parkinson's disease. Complex regulatory interactions were observed among lncRNAs, miRNAs, and biomarkers; for instance, four lncRNAs (NEAT1, AP000766.1, LINC02381, XIST) regulated PGD via hsa-let-7e-5p. Additionally, 29 transcription factors (e.g., STAT1, BRD3, HDAC1, CBFB) co-regulated both biomarkers. Finally, 41 drugs (e.g., cobimetinib fumarate, selumetinib sulfate) were predicted to target MAP2K2, while three (penicillamine, pralmorelin, phenobarbital) targeted PGD. In summary, MAP2K2 and PGD serve as CHD biomarkers, offering new insights into disease pathogenesis.

Introduction

Coronary heart disease (CHD) remains a globally widespread chronic disorder, associated with high rates of illness and death [1]. The disease entity is characterized by insufficient blood supply or obstruction of the coronary arteries, leading to myocardial ischemia, hypoxia, angina pectoris, palpitations, shortness of breath and fatigue; it may also present with other symptoms [2]. In severe cases, it can cause myocardial infarction or arrhythmia, and even be life-threatening [2]. A Atherosclerosis Risk in Communities (ARIC) study found approximately 60500 new myocardial infarctions and 200,000 recurrent events every year between 2005 and 2014 [3]. The pathogenesis of CHD is complex and among the main causes of CHD, atherosclerosis has been widely regarded as the main factor [4]. Inflammation, endothelial dysfunction, hypertension, dyslipidemia, insulin resistance, environmental exposures, and pathogens all contribute to endothelial injury, which in turn contributes to the formation and progression of atherosclerotic plaques [5]. The development of a CHD diagnosis depends on clinical symptoms, physical examination and imaging characteristics (such as electrocardiogram, echocardiogram, coronary angiography, etc) [6, 7]. In current therapies, pharmacological agents, which include antiplatelets, statins, β-blockers, etc, are used along with interventional treatments, such as primary coronary intervention (PCI) and coronary artery bypass surgery (CABG) [8, 9]. However, there are some issues with these treatments. For example, drugs may be ineffective or cause resistance in certain patient populations, and vascular stent technology still suffers from many complications, including in-stent restenosis, late thrombosis, artery injury, and high re-occlusion rates [10]. In recent years, some scientists believe that to develop novel therapeutic targets and therapies for CHD, an in-depth understanding of the

disease's pathogenesis is vital. In particular, research on biomarkers can help early diagnosis of CHD, assess the severity of the disease, predict prognosis, and guide individualized therapeutic strategies.

Secreted predominantly by the pineal gland nocturnally, ME, an endogenous hormone, modulates circadian rhythms and the sleep - wake cycle [11]. Additionally, ME controls various physiological processes, including anti-inflammation, antioxidant, immune regulation, and so on [12]. In the past few years, there has been much research into how CHD may be related to ME. Some research suggests that ME may be associated with the development and risk of CHD [13, 14]. For example, ME can improve ischemia in patients with ST-segment elevation myocardial infarction, and calculation of left ventricular mass by Cardiac Magnetic Resonance (CMR) showed better outcomes in the melatonin group than in the placebo group [15]. Moreover a study found that patients with CHD have reduced nocturnal ME secretion compared with healthy patients, although there are large differences between individuals in the rate of ME secretion pattern [16]. Results from some studies suggest that low ME production is most closely related to CHD, infarction, and congestive heart failure [17, 18]. Nevertheless, the specific mechanism by which ME promotes CHD remains unclear, it is vital to study the role of ME in the progression of CHD, which could present new perspectives on the prevention, diagnosis and treatment of CHD.

This study is based on transcriptome-related data on CHD in the GEO database, melatonin-related biomarkers in CHD were identified through differential analysis, machine learning, etc. Then, we conducted correlation analysis, functional enrichment analysis, regulatory network construction and drug prediction for the above genes. These findings offer novel perspectives for the clinical management of CHD.

Results

Acquisition of 102 candidate genes

The 881 CHD-DEGs were identified, with 677 CHD-DEGs showing up-regulation and 204 CHD-DEGs showing down-regulation in CHD samples compared to control samples (**Figure 1a-b**). MERGs scores were significantly different between the two groups, indicating that ME was associated with the occurrence of CHD ($p < 0.05$) (**Figure 1c**). The cluster analysis conducted revealed no outliers in the GSE179789 dataset (**Figure 1d**). The β was set to 27 when the ordinate scale-free R2 approaches the threshold of 0.85. The mean connectivity also converges towards zero, indicating that the network tends towards a scale-free distribution (**Figure 1e**). Then the nine modules were acquired (**Figure 1f**). The correlation coefficient of module MEblack and MERGs was -0.55 ($p < 0.05$), with the strongest significant correlation (**Figure 1g**). Therewith, the 185 ME-related module genes were obtained from this module. Whereafter, the intersection of 881 CHD-DEGs and 185 ME-related module genes resulted in the identification of 102 candidate genes.(**Figure 2a**). Among the findings of the GO analysis, enrichment of candidate genes was observed in processes such as Golgi vesicle transport, vesicle organization,

secretory granule membrane, and cadherin binding, etc. (**Figure 2b**). Among the KEGG pathways, candidate genes were significantly enriched in Long-term potentiation, Insulin signaling pathway, Salmonella infection, and Phospholipase D signaling pathway (**Figure 2c**).

Screening of candidate biomarkers

After removing the discrete proteins, a PPI network of 58 proteins was built, including 58 nodes and 53 edges (**Figure 3a**). Then, ARAF, RRAS, ACTR1A, ARF3, RAPGEF1, MAP2K2, RALGDS, ACO2, GGA3, PGD, FLNA were the top 11 genes in the Degree algorithm (the scores of genes ACTR1A, RAPGEF1, MAP2K2, RALGDS, GGA3, PGD and FLNA were consistent, so 11 genes were selected) (**Figure 3b**). These 11 genes were input into the LASSO regression model, and finally four candidate biomarkers with regression coefficients not penalized as 0 were obtained, namely RRAS, MAP2K2, RALGDS and PGD (**Figure 3c-d**).

MAP2K2 and PGD were dependable biomarkers for CHD

In the GSE179789 and GSE113079 datasets, boxplots depicted the biomarker expression levels in CHD and control samples, respectively (**Figure 4a-b**). Notably, two candidate biomarkers, MAP2K2 and PGD, exhibited similar expression patterns, showed significant differential expression in both datasets and were subsequently employed for diagnostic validation. The GSE179789 dataset exhibited AUC values of MAP2K2 (AUC = 0.969) and PGD (AUC = 0.969), respectively (**Figure** 4**c**). In the GSE113079 dataset, the AUC values for MAP2K2 and PGD were observed to be 0.737 and 0.805 (**Figure 4d**). The AUC values of MAP2K2 and PGD exceeded 0.7, suggesting that they exhibit strong diagnostic efficacy as biomarkers. The hidden layer was set to 3, and the ANN model was constructed based on two biomarkers in GSE179789 and GSE113079 (**Figure 4e-f**). The AUC values of the models exceeded 0.7, indicating a significant level of accuracy in the model constructed using the biomarkers MAP2K2 and PGD, which further proved the predictive accuracy of biomarkers (**Figure 4g-h**).

MAP2K2 and PGD were enriched in ribosome, prion diseases, Parkinson's disease, etc.

The expression of MAP2K2 and PGD correlated significantly and positively ($R = 0.70$, $p < 0.05$) (**Figure 5a**). And they interacted with 20 genes such as MAPK1, KSR1, PGLS, RPE and so on in glucose 6-phosphate metabolic process, organelle inheritance, NADPH regeneration, pentose-phosphate shunt, and Golgi inheritance functions (**Figure 5b**). MAP2K2 was enriched in 53 pathways, such as ribosome, protein export, and prion diseases (**Figure 5c**, **Supplementary Table 2**). GSEA enrichment analysis revealed significant correlations between PGD with B-cell receptor signaling pathway, Leishmania infection, acute myeloid leukemia, and other pathways (**Figure 5d**, **Supplementary Table 3**). They were all enriched in the ribosome, prion diseases, Parkinson's disease, etc.

There were intricate regulatory relationships between lncRNA, miRNA, and mRNA

Totally, 45 miRNAs were predicted in TarBase, and 47 were predicted in miRTarBase. Then, 10 key miRNAs were shared by the two databases. Among them, the nine key miRNAs corresponded to eight lncRNAs. LncRNA, miRNA, and mRNA were engaged in elaborate post - transcriptional regulatory crosstalk (**Figure 6a**). For example, four lncRNAs regulated (NEAT1, AP000766.1, LINC02381, XIST) PGD by hsa-let-7e-5p. MAP2K2 predicted 40 TFs and PGD predicted 36 TFs to construct the TF-mRNA network, of which 29 TFs were predicted by both biomarkers, such as STAT1, BRD3, HDAC1, and CBFB (**Figure 6b**). MAP2K2 searched 41 target drugs, such as COBIMETINIB FUMARATE and SELUMETINIB SULFATE. And PGD predicted three drugs: PENICILLAMINE, PRALMORELIN, and PHENOBARBITAL (**Figure 6c**).

The expression of biomarkers in clinical samples was consistent with the dataset

The results of RT-qPCR revealed that MAP2K2 and PGD were markedly up-regulated in clinical CHD samples, which was consistent with the findings of the datasets (**Figure 7a-b)**.

Discussion

CHD, also known as coronary atherosclerotic heart disease, ranks among the most enormous burdens for public health and the economy of the low-income and lower-middle-income nations [19]. The main cause of CHD is atherosclerosis, which is characterized by the deposition of plaques of fatty material within the arteries. As a result of plaque development in coronary arteries and a blockage or narrowing of the vessels, CHD occurs [20, 21]. Some studies have shown that circulating ME levels are altered in patients with CHD. For example, there is an independent relationship between nocturnal oxidized low-density lipoprotein and melatonin levels in patients with myocardial infarction [22]. Inadequate sleep or poor sleep quality may increase the risk of CHD, and melatonin secretion is closely related to sleep [23, 24]. Low serum ME levels have been reported in individuals, which exacerbates the possibility of ischemia-reperfusion injury leading to further cardiac damage, as melatonin has been described as a direct free radical scavenger that is highly effective in preventing reactive oxygen and nitrogen damage [13]. Several studies have shown the beneficial effects of ME supplementation on biomarkers of oxidative stress and inflammation, blood pressure, glycemic control, and lipids in animal models and patients with T2DM and MetS [25, 26]. To further explore the relationship between ME and CHD, by utilizing bioinformatic techniques, two MRGs (MAP2K2, PGD) in patients with CHD were identified in the present study, which may offer a new perspective for treating CHD.

MAP2K2 (Mitogen-Activated Protein Kinase Kinase 2) is a key component of the MAPK signaling pathway. This gene encodes a dual-specificity kinase that activates downstream MAP kinases in response to extracellular stimuli [27]. Continuous activation of MAPK signaling due to Ras pathway dysfunction can lead to endothelial cell dysfunction and speed up atherosclerosis progression. Several studies have suggested that mutations or deletions in the MAP2K2 gene may be implicated in the etiology of RASopathies, a collection of developmental disorders resulting from mutations in genes encoding components of the RAS-MAPK pathway [28]. Proliferation, differentiation, growth, aging and deaths of cells depend on the MAPK signaling pathway, meanwhile it plays an essential role in atherosclerosis, which is the underlying pathogenesis of CHD [29]. During the onset and development of atherosclerosis, MAP2K2, which is an important member of the MAPK pathway, expression level increased result in inflammation via activation downstream MAPK pathway factors such as ERK phosphorylation [30]. In the meantime, inflammatory responses are amplified through activation of the MAP2K/ERK pathway and the expression of various cytokines, which may damage the vascular system [31]. MAP2K2 indirectly phosphorylates ERK by upregulating lnc_000048 and ultimately activates the inflammatory response through MAPK pathways, reducing plaque stability [32]. According to some studies, MAP2K2 expression is significantly suppressed in patients with metabolic syndrome, which is associated with an increased risk of cardiovascular disease, type 2 diabetes (DM), and cardiovascular-specific mortality [33]. As MAP2K2 is metabolized through the MAPK signaling pathway, it may affect cardiovascular disease (CVD), including CHD. According to the qPCR results of this study, the upregulation of map2k2 expression in the disease group was in agreement with the bioinformatics analysis findings. Given that MAP2K2 is metabolized through the MAPK signaling pathway, it is speculated that MAP2K2 may affect cardiovascular diseases, including CHD.

PGD (Phosphogluconate Dehydrogenase) also referred to as 6PGD, is the third enzyme of the pentose phosphate pathway (PPP) that catalyzes 6-phosphogluconate (6-PG) degradation into ribulose-5-phosphate (Ru-5-P) while simultaneously reducing NADP + to NADPH [34]. A study has found that Ru-5-P derived from PGD inhibits 5'-adenosine monophosphate-activated protein kinase (AMPK) by destroying the upstream LKB1 complex, thereby increasing fatty acid synthesis, especially saturated fatty acids (SFA) [35]. The effects of fatty acids on CVD are thought to lie in multiple mechanisms, such as cardio-metabolism, lipo-toxicity, electromechanical properties of cardiomyocytes, and inflammatory processes [36]. This suggests that PGD may influence the onset and progression of cardiovascular diseases, including CHD, by participating in the synthesis of fatty acids. This finding could offer valuable insights for diagnosis and treatment of CHD.

This research found that GSEA enrichment analysis indicated MAP2K2 and PGD were involved in signaling pathways like ribosomes, prion diseases, and Parkinson's disease. These pathways are frequently enriched in the context of these biomarkers. Ribosome, composed of RNA and proteins, are increasingly recognized for their important roles in cell function, responses to stimuli, and disease development. Proteins involved in ribosome biogenesis play a crucial role in regulating cell growth and proliferation [36]; disruption of this process can result in aberrant cell proliferation and the development

of pathological conditions, including cancer and metabolic disorders [37]. Some studies have shown that ribosomal proteins (RPs) have been linked to the development of cardiovascular disease [38, 39]. Smolock EM56, et al. discovered that L17, functioning as a ribosomal protein, serves as a potent inhibitor of vascular smooth muscle cell growth, effectively impeding the thickening of the intimal layer in the mouse carotid artery. The expression of L17 hinders the proliferation of vascular smooth muscle cells by inducing cell cycle arrest in the G0/G1 phase. S6K, a ribosomal protein, is a prominent downstream effector of mTOR (mammalian target of rapamycin) and plays a crucial role in various cardiovascular and metabolic processes [40]. Research indicates that following myocardial infarction, S6K is rapidly and robustly activated, contributing to maladaptive cardiac remodeling via heightened Akt signaling in the infarcted myocardium [41]. The study revealed that MAP2K2 is enriched in the ribosomal signaling pathway, indicating it might influence the protein synthesis process linked to cardiovascular diseases, leading to abnormal expression of proteins essential for the cardiovascular system's normal function, such as influencing proteins involved in vasodilation and contraction, or altering the expression of proteins associated with the structure and function of heart muscle cells, thereby disturbing the cardiovascular system's equilibrium, as a result, it causes or exacerbates CHD.

There has also been an increased interest in the potential link between cardiovascular disease and Parkinson's disease in recent years. It has also been reported that many of the potential risk factors for Parkinson's disease are also typically cardiovascular risk factors (such as advanced age, male sex, diabetes, HTN, and obesity), and that there are common mechanistic hypotheses for both diseases (such as chronic inflammation and oxidative stress) [42, 43]. Despite this, there is still no clear conclusion regarding how cardiovascular disease and Parkinson's disease are related. There is an increasing agreement among researchers that the risk of cardiovascular disease in patients with Parkinson's disease significantly rises as the disease advances. Using data from two different populations, Li et al found that stroke and coronary artery disease (CAD) may contribute to Parkinson's disease (PD) pathogenesis [44]. Liang et al. found that the risk of myocardial infarction in PD patients was significantly elevated [45]. Another study found that among newly diagnosed PD patients, 62.5% had moderate to high cardiovascular risk, which was higher than the general population [46]. These studies further support the hypothesis that cardiovascular disease is associated with Parkinson's disease. However, several opinions have suggested that PD does not increase the overall risk of myocardial infarction and cardiovascular death, and that there is no difference in the risk of myocardial infarction and cardiovascular death between PD and non-PD individuals [47, 48]. Even meta-analysis suggests that PD is associated with a reduced risk of MI [49]. Therefore, more research is needed to prove the link between PD and CVD. Our study provides a reference for the study of the mechanism of action of MRGs in CHD.

According to the study, 29 transcription factors were co-regulated by two biomarkers, namely STAT1, BRD3, HDAC1, and CBFB. In the immune response, STAT1, activated by the IFN-γ/JAK2 pathway [50], contributes by regulating the activation of immune cells, secretion of inflammatory factors, and expression of inflammatory genes [51, 52]. It was found in the study that the STAT1 promoter's

methylation level was significantly reduced in coronary heart disease patients compared to the control group [53]. The binding site (GAS/ISRE) was notably enriched in the promoter region of genes related to plaque (CCL2/5/19, VEGFC, etc.), indicating its role in plaque formation through the regulation of cell adhesion, migration, and inflammation [54]. This investigation proposes that the progression of coronary heart disease could be impacted by map2k2 and PGD via the modulation of the STAT1 signaling axis.

Identified as potential biomarkers and therapeutic targets for CHD, these two genes could revolutionize the approach to diagnosing and treating CHD patients, paving the way for precision medicine in this field. However, based on bioinformatics analysis of public databases, this study needs further testing to investigate the mechanism of action of biomarkers and more clinical studies to verify its results.

Materials and methods

Data collection

The Gene Expression Omnibus (GEO) (https://www.ncbi.nlm.nih.gov/geo/) database offered the retrieve of the GSE179789 (GPL570) and GSE113079 (GPL20115) datasets related to CHD. The GSE179789 dataset, which included 8 CHD patients and 8 controls with peripheral blood monocyte (PBMC) samples, served as the training set. In contrast, the validation set, GSE113079, contained PBMC samples of 93 CHD patients and 48 controls. We obtained 12 ME - related genes (MERGs) from the literature [55] , that is, MTNR1A, MTNR1B, GPR50, AANAT, ASMT, CYP1A2, CYP2C19, RORA, PER2, PER3, ARNTL, and CLOCK.

Differential Analysis

For the identification of CHD-differentially expressed genes (DEGs) between two groups within the training set, differential analysis was conducted using the limma package (V 3.52.4) [56]. $|log2FoldChange(FC)| > 0.5$, $p < 0.05$ was used as the screening criterion. The generation of volcano plots was facilitated by the ggplot2 package (V 3.4.1) [57]. Additionally, heat maps were constructed to visualize the expression patterns of CHD-DEGs in control and CHD samples by utilizing the ComplexHeatmap package (V 2.14.0) [58].

Weighted gene co-expression network analysis (WGCNA)

The scores of the 12 MERGs were first calculated in different samples of the GSE179789 dataset by the GSVA package (V 1.42.0) [59] . The score of MERGs was used as a trait, and the R package WGCNA (V 1.71) [60] was used for analysis to screen the modules and genes related to the trait. Firstly, prior to clustering, gene expression values were screened, and only genes with expression values above 1 were selected for sample cluster analysis. The sample cluster analysis was adopted to identify any outlier

samples that may need to be excluded to ensure the accuracy of subsequent analyses. Secondly, to maximize the scale - free distribution of gene interactions, the soft threshold (β) was determined. With the hybrid dynamic tree - cutting algorithm as the clustering criterion, module partitioning was carried out. The procedure was parameterized by β and constrained each module to have a minimum of 50 genes. Thereafter, by computing the correlation coefficients between each module and the MRGs score, we aimed to determine the module that had the strongest association with MRGs. Finally, we obtained ME-related module genes in the most relevant module.

Identification and functional enrichment analysis of candidate genes

The CHD-DEGs and ME-related module genes were intersected using ggvenn (V 0.1.9)[61] to acquired candidate genes. The cluster Profiler package (V 4.7.1.3) [62] was applied to conduct Gene Ontology (GO) and Kyoto Encyclopedia of Genes and Genomes (KEGG) pathway enrichment analyses of the candidate genes, aiming to identify common functions and related pathways among them [63-65].

Establishment of protein-protein interaction (PPI) network and least absolute shrinkage and selection operator (LASSO) analysis

A PPI network of the candidate genes was constructed by the STRING website (http://string.embl.de/) to investigate the interaction among the candidate genes (confidence score = 0.5). Hereafter, the Degree algorithm in cytoHubba, a built-in plugin of Cytoscape (V 3.8.2) [66], was leveraged to determine the connectivity score of each gene. Subsequently, the top 10 genes were selected for LASSO method by glmnet package (V 4.1.4) [67]. Genes whose regression coefficients were not penalized to zero when the optimal lambda was reached in the LASSO regression model were regarded as candidate biomthearkers.

Expression level verification and Receiver Operating Characteristic (ROC) analysis

The GSE179789 and GSE113079 datasets were adopted to compare the expression of candidate biomarkers in CHD patients and controls. Meanwhile, candidate biomarkers that exhibited consistent expression trends and significant distinctions between the groups in both datasets were screened for ROC analysis ($p < 0.05$). In detail, the area under the curve (AUC) values were determined to quantitatively measure the diagnostic accuracy of the genes, and genes with an AUC exceeding 0.7 were considered reliable biomarkers.

Artificial Neural Network (ANN) and correlation analysis

Aiming further to validate the overall disease diagnosis results of biomarkers, the neuralnet package (V 1.44.2) [68] was utilized to construct ANN models based on biomarkers in GSE179789 and GSE113079. Subsequently, the diagnostic ability of the model was assessed by plotting an ROC curve. Furthermore, in the GSE179789 dataset, Spearman correlation analyzed biomarker expression correlations.

Gene set enrichment analysis (GSEA) and gene-gene interaction (GGI) network

To understand the biological characteristics of these biomarkers, we utilized GeneMANIA (http://www.genemania.org/) to construct and analyze a GGI network between the biomarkers and their co-expressed genes.

We performed GSEA pathway enrichment analysis according to biomarkers to delve deeper into the associated functions. Concretely, according to their biomarker levels, CHD samples from GSE179789 were partitioned into two distinct subsets: those with high biomarker expression and those with low biomarker expression. The limma package (V 3.52.4) [56] was used for differential analysis based on high and low expression groups, and log2FC of obtained genes was calculated. The log2FC was sorted from largest to smallest, after which GSEA was carried out by the clusterProfiler package (V 4.7.1.3) ($|NES| > 1$, $p < 0.05$) [62] . The “c2. cp.kegg.v2023.1. Hs.symbols.gmt” as the reference gene set in the Molecular Signatures Database (MSigDB, https://www.gsea-msigdb.org/gsea/msigdb).

Construction of regulatory network and drug prediction

Transcription factors (TFs) against biomarkers were forecasted employing the hTFtarget database (http://bioinfo.life.hust.edu.cn/hTFtarget), and datasets greater than 1 were screened. Similarly, TarBase (http://www.diana.pcbi.upenn.edu/tarbase) and miRTarBase (http://miRTarBase.mbc.nctu.edu.tw/) databases were utilized for the prediction of miRNA biomarkers, with the intersection of these two databases results as key miRNAs. Subsequently, the Starbase database (http://starbase.sysu.edu.cn/) was implemented to predict the lncRNAs targeted by key miRNAs. In an effort to discover novel medications for CHD treatment, the Drug-Gene Interaction Database (DGIdb, http://www.dgidb.org) was queried to retrieve drugs that specifically target the key biomarkers. Ultimately, the Cytoscape (V 3.8.2) [66] was utilized to present the lncRNA-miRNA-mRNA, TF-mRNA, and mRNA-drug networks.

Validation of biomarker expression in clinical samples

To assess biomarker expression in clinical samples, we procured five pairs of blood samples from the Jiangxi Provincial People’s Hospital for reverse transcription quantitative polymerase chain reaction (RT-

qPCR) analysis, comprising five control and five CHD samples. The patients included were those admitted to Jiangxi Provincial People's Hospital from January 1, 2024, to January 31, 2024. All human research procedures were performed in accordance with the Declaration of Helsinki and the relevant guidelines and regulations approved by Medical Ethics Committee of Jiangxi Provincial People's Hospital (Approval Number: Kekuai 2023(15)- Project). Informed consent was obtained from all participants and/or their legal guardians prior to the study initiation. Total RNA was extracted from the samples with TRIzol reagent (Ambion, Austin, USA) following the manufacturer's instructions. Subsequently, cDNA synthesis was performed using the SureScript First-strand cDNA synthesis kit (Servicebio, Wuhan, China), following the instructions. For RT-qPCR analysis, the 2x Universal Blue SYBR Green qPCR Master Mix (Servicebio) was utilized. **Supplenemntary Table 1** provides the primer sequences employed for PCR amplification. Biomarker expression levels were quantified using the $2^{-\Delta\Delta Ct}$ method [69].

Statistical analysis

Data analysis was performed using R (version 4.2.2), with statistical significance defined as $p < 0.05$.

Abbreviations

Abbreviation	Full Term
ME	Melatonin
CHD	Coronary Heart Disease
DEGs	Differentially Expressed Genes
GSEA	Gene Set Enrichment Analysis
RT-qPCR	Reverse Transcription-quantitative Polymerase Chain Reaction
AUC	Area Under the Curve
ROC	Receiver Operating Characteristic
ANN	Artificial Neural Network
PPI	Protein-Protein Interaction
LASSO	Least Absolute Shrinkage and Selection Operator
WGCNA	Weighted Gene Co-expression Network Analysis
GO	Gene Ontology
KEGG	Kyoto Encyclopedia of Genes and Genomes
GGI	Gene-Gene Interaction
TF	Transcription Factor
miRNA	MicroRNA
lncRNA	Long Non-coding RNA
MAP2K2	Mitogen-Activated Protein Kinase Kinase 2
PGD	Phosphogluconate Dehydrogenase
PPP	Pentose Phosphate Pathway
NADPH	Nicotinamide Adenine Dinucleotide Phosphate
AMPK	5'-Adenosine Monophosphate-activated Protein Kinase
mTOR	Mammalian Target of Rapamycin
STAT1	Signal Transducer and Activator of Transcription 1
ERK	Extracellular Signal-regulated Kinase
MAPK	Mitogen-Activated Protein Kinase
CVD	Cardiovascular Disease
PBMC	Peripheral Blood Mononuclear Cell

GEO	Gene Expression Omnibus
GSVA	Gene Set Variation Analysis
MSigDB	Molecular Signatures Database
DGIdb	Drug-Gene Interaction Database

Declarations

Competing interests

"The authors declare that the research was conducted in the absence of any commercial or financial relationships that could be construed as a potential conflict of interest."

Funding

This research received no specific grant from funding agencies in the public, commercial, or not-for-profit sectors.

Author Contribution

Yongchao Peng: Data curation, Validation, Visualization, Writing–review & editing. Xuemin Zhou: Validation, Writing–review & editing. Li Huang: Data curation, Investigation, Resources, Visualization. Yaowu Xie: Conceptualization, Project administration, Supervision, Writing–review & editing. Xuanlan Chen: Conceptualization, Supervision, Writing–review & editing. Zhifeng Zhang: Conceptualization, Data curation, Validation, Visualization, Writing–original draft, Writing–review & editing. This work currently described has not been published, is not being considered for publication elsewhere, and its publication was approved by all authors.

Acknowledgments

We would like to express our sincere gratitude to all individuals and organizations who supported and assisted us throughout this research. Special thanks to the following authors: Yongchao Peng, Xuemin Zhou, Xuanlan Chen, Yaowu Xie, Zhifeng Zhang. In conclusion, we extend our thanks to everyone who has supported and assisted us along the way. Without your support, this research would not have been possible.

Data Availability

The datasets GSE179789 and GSE113079 for this study can be found in the Gene Expression Omnibus (GEO) (https://www.ncbi.nlm.nih.gov/geo/).

References

1. Townsend, N. *et al.* Epidemiology of cardiovascular disease in Europe. *Nat Rev Cardiol* **19,** 133-143, (2022).
2. Byrne, R., Coughlan, J. J., Rossello, X., Ibanez, B. & Members of the Task Force for the, E. S. C. G. f. t. m. o. a. c. s. Key priorities for the implementation of the 2023 ESC Guidelines for the management of acute coronary syndromes in low-resource settings. *Eur Heart J Qual Care Clin Outcomes*, (2025).
3. Tsao, C. W. *et al.* Heart Disease and Stroke Statistics-2023 Update: A Report From the American Heart Association. *Circulation* **147,** e93-e621, (2023).
4. Stark, K. & Massberg, S. Interplay between inflammation and thrombosis in cardiovascular pathology. *Nat Rev Cardiol* **18,** 666-682, (2021).
5. Hansson, G. K. Inflammation, atherosclerosis, and coronary artery disease. *N Engl J Med* **352,** 1685-1695, (2005).
6. Smith, S. C., Jr. *et al.* AHA/ACCF Secondary Prevention and Risk Reduction Therapy for Patients with Coronary and other Atherosclerotic Vascular Disease: 2011 update: a guideline from the American Heart Association and American College of Cardiology Foundation. *Circulation* **124,** 2458-2473, (2011).
7. Bittner, V. The New 2019 AHA/ACC Guideline on the Primary Prevention of Cardiovascular Disease. *Circulation* **142,** 2402-2404, (2020).
8. Virani, S. S. *et al.* 2023 AHA/ACC/ACCP/ASPC/NLA/PCNA Guideline for the Management of Patients With Chronic Coronary Disease: A Report of the American Heart Association/American College of Cardiology Joint Committee on Clinical Practice Guidelines. *Circulation* **148,** e9-e119, (2023).
9. Collet, J. P. *et al.* 2020 ESC Guidelines for the management of acute coronary syndromes in patients presenting without persistent ST-segment elevation. *Eur Heart J* **42,** 1289-1367, (2021).
10. Rajagopalan, S. & Rashid, I. Regression therapy for cardiovascular disease. *Eur Heart J* **40,** 3418-3420, (2019).
11. Wongchitrat, P., Shukla, M., Sharma, R., Govitrapong, P. & Reiter, R. J. Role of Melatonin on Virus-Induced Neuropathogenesis-A Concomitant Therapeutic Strategy to Understand SARS-CoV-2 Infection. *Antioxidants (Basel)* **10**, (2021).
12. Dawson, D. & Encel, N. Melatonin and sleep in humans. *J Pineal Res* **15,** 1-12, (1993).
13. Pandi-Perumal, S. R. *et al.* Melatonin and Human Cardiovascular Disease. *J Cardiovasc Pharmacol Ther* **22,** 122-132, (2017).
14. Dominguez-Rodriguez, A., Abreu-Gonzalez, P., Sanchez-Sanchez, J. J., Kaski, J. C. & Reiter, R. J. Melatonin and circadian biology in human cardiovascular disease. *J Pineal Res* **49,** 14-22, (2010).

15. Dominguez-Rodriguez, A. *et al.* Usefulness of Early Treatment With Melatonin to Reduce Infarct Size in Patients With ST-Segment Elevation Myocardial Infarction Receiving Percutaneous Coronary Intervention (From the Melatonin Adjunct in the Acute Myocardial Infarction Treated With Angioplasty Trial). *Am J Cardiol* **120,** 522-526, (2017).
16. Yaprak, M. *et al.* Decreased nocturnal synthesis of melatonin in patients with coronary artery disease. *Int J Cardiol* **89,** 103-107, (2003).
17. Dominguez-Rodriguez, A., Abreu-Gonzalez, P., Piccolo, R., Galasso, G. & Reiter, R. J. Melatonin is associated with reverse remodeling after cardiac resynchronization therapy in patients with heart failure and ventricular dyssynchrony. *Int J Cardiol* **221,** 359-363, (2016).
18. Su, H. *et al.* Correlations of Serum Cyclophilin A and Melatonin Concentrations with Hypertension-induced Left Ventricular Hypertrophy. *Arch Med Res* **48,** 526-534, (2017).
19. Zhou, Y. *et al.* The Role of the VEGF Family in Coronary Heart Disease. *Front Cardiovasc Med* **8,** 738325, (2021).
20. Zhu, K. F., Wang, Y. M., Zhu, J. Z., Zhou, Q. Y. & Wang, N. F. National prevalence of coronary heart disease and its relationship with human development index: A systematic review. *Eur J Prev Cardiol* **23,** 530-543, (2016).
21. Si, R. *et al.* Overexpression of p53 due to excess protein O-GlcNAcylation is associated with coronary microvascular disease in type 2 diabetes. *Cardiovasc Res* **116,** 1186-1198, (2020).
22. Dominguez-Rodriguez, A. *et al.* Elevated levels of oxidized low-density lipoprotein and impaired nocturnal synthesis of melatonin in patients with myocardial infarction. *Atherosclerosis* **180,** 101-105, (2005).
23. Covassin, N. & Somers, V. K. Sleep, melatonin, and cardiovascular disease. *Lancet Neurol* **22,** 979-981, (2023).
24. Zisapel, N. New perspectives on the role of melatonin in human sleep, circadian rhythms and their regulation. *Br J Pharmacol* **175,** 3190-3199, (2018).
25. Peschke, E. *et al.* The insulin-melatonin antagonism: studies in the LEW.1AR1-iddm rat (an animal model of human type 1 diabetes mellitus). *Diabetologia* **54,** 1831-1840, (2011).
26. Kozirog, M. *et al.* Melatonin treatment improves blood pressure, lipid profile, and parameters of oxidative stress in patients with metabolic syndrome. *J Pineal Res* **50,** 261-266, (2011).
27. Gos, M. *et al.* MAP2K2 mutation as a cause of cardio-facio-cutaneous syndrome in an infant with a severe and fatal course of the disease. *Am J Med Genet A* **176,** 1670-1674, (2018).
28. Nowaczyk, M. J. *et al.* Deletion of MAP2K2/MEK2: a novel mechanism for a RASopathy? *Clin Genet* **85,** 138-146, (2014).
29. Roskoski, R., Jr. MEK1/2 dual-specificity protein kinases: structure and regulation. *Biochem Biophys Res Commun* **417,** 5-10, (2012).
30. Kent, O. A. *et al.* Haploinsufficiency of RREB1 causes a Noonan-like RASopathy via epigenetic reprogramming of RAS-MAPK pathway genes. *Nat Commun* **11,** 4673, (2020).

31. Sarkar, A., Chamucero-Millares, J. A. & Rojas, M. Romulus and Remus of Inflammation: The Conflicting Roles of MAP2K1 and MAP2K2 in Acute Respiratory Distress Syndrome. *Am J Respir Cell Mol Biol* **66,** 479-480, (2022).
32. Zhang, S. *et al.* Lnc_000048 Promotes Histone H3K4 Methylation of MAP2K2 to Reduce Plaque Stability by Recruiting KDM1A in Carotid Atherosclerosis. *Mol Neurobiol* **60,** 2572-2586, (2023).
33. Tabur, S. *et al.* Evidence for elevated (LIMK2 and CFL1) and suppressed (ICAM1, EZR, MAP2K2, and NOS3) gene expressions in metabolic syndrome. *Endocrine* **53,** 465-470, (2016).
34. Hanau, S., Montin, K., Cervellati, C., Magnani, M. & Dallocchio, F. 6-Phosphogluconate dehydrogenase mechanism: evidence for allosteric modulation by substrate. *J Biol Chem* **285,** 21366-21371, (2010).
35. Lin, R. *et al.* 6-Phosphogluconate dehydrogenase links oxidative PPP, lipogenesis and tumour growth by inhibiting LKB1-AMPK signalling. *Nat Cell Biol* **17,** 1484-1496, (2015).
36. Soppert, J., Lehrke, M., Marx, N., Jankowski, J. & Noels, H. Lipoproteins and lipids in cardiovascular disease: from mechanistic insights to therapeutic targeting. *Adv Drug Deliv Rev* **159,** 4-33, (2020).
37. Ruggero, D. & Pandolfi, P. P. Does the ribosome translate cancer? *Nat Rev Cancer* **3,** 179-192, (2003).
38. Alexander, S. J., Woodling, N. S. & Yedvobnick, B. Insertional inactivation of the L13a ribosomal protein gene of Drosophila melanogaster identifies a new Minute locus. *Gene* **368,** 46-52, (2006).
39. Casad, M. E. *et al.* Cardiomyopathy is associated with ribosomal protein gene haplo-insufficiency in Drosophila melanogaster. *Genetics* **189,** 861-870, (2011).
40. Hay, N. & Sonenberg, N. Upstream and downstream of mTOR. *Genes Dev* **18,** 1926-1945, (2004).
41. Di, R. *et al.* S6K inhibition renders cardiac protection against myocardial infarction through PDK1 phosphorylation of Akt. *Biochem J* **441,** 199-207, (2012).
42. Scorza, F. A., Fiorini, A. C., Scorza, C. A. & Finsterer, J. Cardiac abnormalities in Parkinson's disease and Parkinsonism. *J Clin Neurosci* **53,** 1-5, (2018).
43. Lang, A. E. & Espay, A. J. Disease Modification in Parkinson's Disease: Current Approaches, Challenges, and Future Considerations. *Mov Disord* **33,** 660-677, (2018).
44. Li, Q., Wang, C., Tang, H., Chen, S. & Ma, J. Stroke and Coronary Artery Disease Are Associated With Parkinson's Disease. *Can J Neurol Sci* **45,** 559-565, (2018).
45. Liang, H. W., Huang, Y. P. & Pan, S. L. Parkinson disease and risk of acute myocardial infarction: A population-based, propensity score-matched, longitudinal follow-up study. *Am Heart J* **169,** 508-514, (2015).
46. Swallow, D. M. *et al.* Statins are underused in recent-onset Parkinson's disease with increased vascular risk: findings from the UK Tracking Parkinson's and Oxford Parkinson's Disease Centre (OPDC) discovery cohorts. *J Neurol Neurosurg Psychiatry* **87,** 1183-1190, (2016).
47. Hu, Y. & Xu, S. Association between Parkinson's disease and the risk of adverse cardiovascular events: a systematic review and meta-analysis. *Front Cardiovasc Med* **10,** 1284826, (2023).
48. Alves, M., Caldeira, D., Ferro, J. M. & Ferreira, J. J. Does Parkinson's disease increase the risk of cardiovascular events? A systematic review and meta-analysis. *Eur J Neurol* **27,** 288-296, (2020).

49. Nabizadeh, F., Valizadeh, P., Sharifi, P., Zafari, R. & Mirmosayyeb, O. Risk of myocardial infarction in Parkinson's disease: A systematic review and meta-analysis. *Eur J Neurol* **30,** 2557-2569, (2023).
50. Liu, Y. *et al.* APLNR Regulates IFN-gamma signaling via beta-arrestin 1 mediated JAK-STAT1 pathway in melanoma cells. *Biochem J* **479,** 385-399, (2022).
51. Tamura, T., Yanai, H., Savitsky, D. & Taniguchi, T. The IRF family transcription factors in immunity and oncogenesis. *Annu Rev Immunol* **26,** 535-584, (2008).
52. Liu, J., Guan, X. & Ma, X. Interferon regulatory factor 1 is an essential and direct transcriptional activator for interferon gamma-induced RANTES/CCl5 expression in macrophages. *J Biol Chem* **280,** 24347-24355, (2005).
53. Bakshi, C., Vijayvergiya, R. & Dhawan, V. Aberrant DNA methylation of M1-macrophage genes in coronary artery disease. *Sci Rep* **9,** 1429, (2019).
54. Sikorski, K., Wesoly, J. & Bluyssen, H. A. Data mining of atherosclerotic plaque transcriptomes predicts STAT1-dependent inflammatory signal integration in vascular disease. *Int J Mol Sci* **15,** 14313-14331, (2014).
55. Zhang, J. *et al.* Pan-cancer analyses reveal genomics and clinical characteristics of the melatonergic regulators in cancer. *J Pineal Res* **71,** e12758, (2021).
56. Ritchie, M. E. *et al.* limma powers differential expression analyses for RNA-sequencing and microarray studies. *Nucleic Acids Res* **43,** e47, (2015).
57. Gustavsson, E. K., Zhang, D., Reynolds, R. H., Garcia-Ruiz, S. & Ryten, M. ggtranscript: an R package for the visualization and interpretation of transcript isoforms using ggplot2. *Bioinformatics* **38,** 3844-3846, (2022).
58. Gu, Z., Eils, R. & Schlesner, M. Complex heatmaps reveal patterns and correlations in multidimensional genomic data. *Bioinformatics* **32,** 2847-2849, (2016).
59. Hänzelmann, S., Castelo, R. & Guinney, J. GSVA: gene set variation analysis for microarray and RNA-seq data. *BMC Bioinformatics* **14,** 7, (2013).
60. Langfelder, P. & Horvath, S. WGCNA: an R package for weighted correlation network analysis. *BMC Bioinformatics* **9,** 559, (2008).
61. Mao, W., Ding, J., Li, Y., Huang, R. & Wang, B. Inhibition of cell survival and invasion by Tanshinone IIA via FTH1: A key therapeutic target and biomarker in head and neck squamous cell carcinoma. *Exp Ther Med* **24,** 521, (2022).
62. Wu, T. *et al.* clusterProfiler 4.0: A universal enrichment tool for interpreting omics data. *Innovation (Camb)* **2,** 100141, (2021).
63. Kanehisa, M., Furumichi, M., Sato, Y., Matsuura, Y. & Ishiguro-Watanabe, M. KEGG: biological systems database as a model of the real world. *Nucleic Acids Res* **53,** D672-d677, (2025).
64. Kanehisa, M. Toward understanding the origin and evolution of cellular organisms. *Protein Sci* **28,** 1947-1951, (2019).

65. Kanehisa, M. & Goto, S. KEGG: kyoto encyclopedia of genes and genomes. *Nucleic Acids Res* **28,** 27-30, (2000).
66. Shannon, P. *et al.* Cytoscape: a software environment for integrated models of biomolecular interaction networks. *Genome Res* **13,** 2498-2504, (2003).
67. Sasikumar, D. *et al.* Caging and photo-triggered uncaging of singlet oxygen by excited state engineering of electron donor-acceptor-linked molecular sensors. *Sci Rep* **12,** 11371, (2022).
68. Li, S. *et al.* Construction of Osteosarcoma Diagnosis Model by Random Forest and Artificial Neural Network. *J Pers Med* **13**, (2023).
69. Livak, K. J. & Schmittgen, T. D. Analysis of relative gene expression data using real-time quantitative PCR and the 2(-Delta Delta C(T)) Method. *Methods* **25,** 402-408, (2001).

Figures

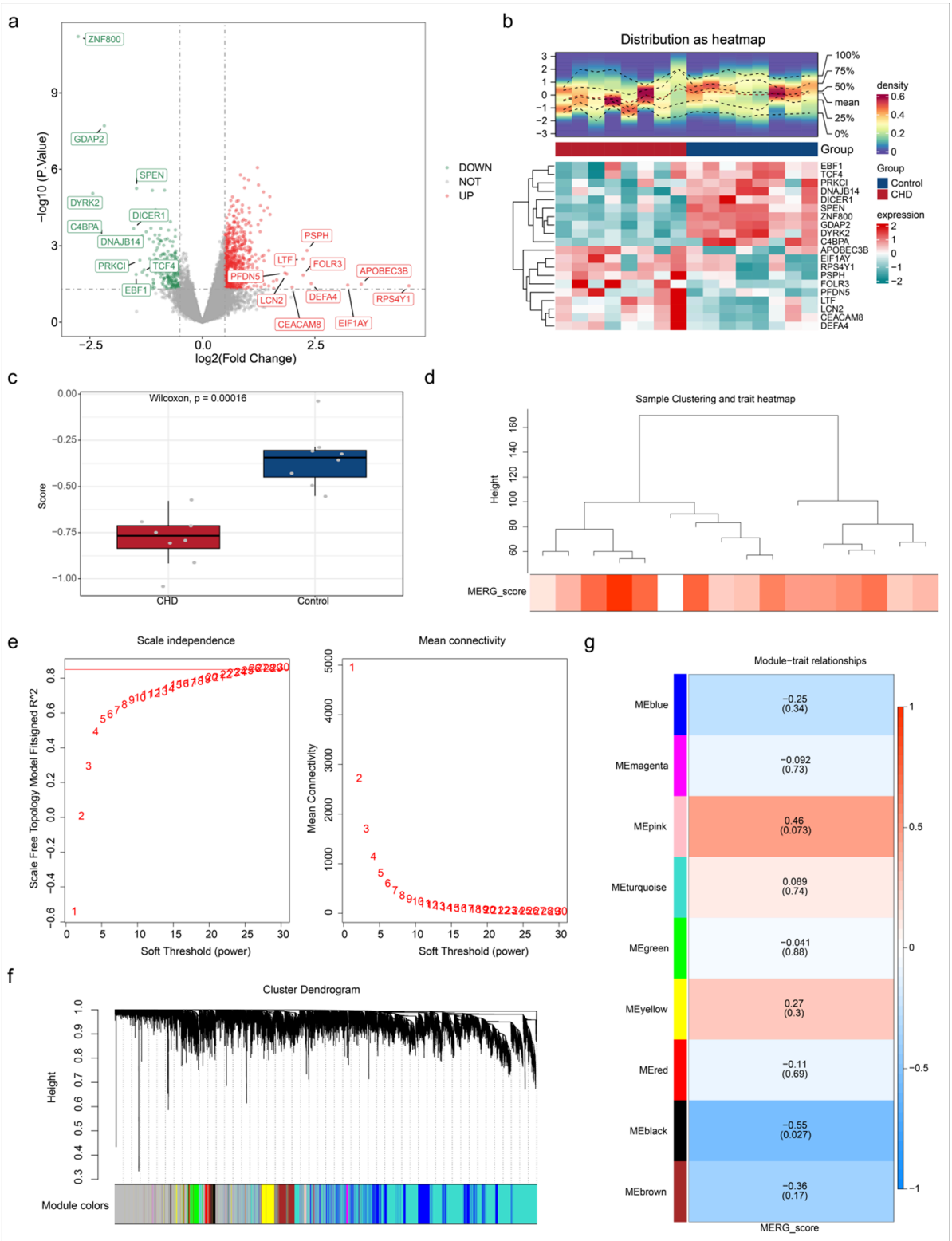


Figure 1

Identification of coronary heart disease (CHD)-related differentially expressed genes (DEGs) and melatonin-associated modules. (**a**) Volcano plot displaying DEGs between CHD and control samples. Red dots represent upregulated genes and blue dots represent downregulated genes; the top 10 genes with the most significant up/downregulation differences are shown. (**b**) Heatmap of DEG expression patterns in CHD and control groups. The top10 upregulated and downregulated gene expression density

heat maps of the samples are shown in the upper part, showing the lines of the five percentiles and the average value; the bottom part is the expression heat map of the top10 upregulated and downregulated genes of the samples. (**c**) Comparison of melatonin-related gene (MERG) scores between CHD and healthy samples. (**d**) Sample clustering dendrogram showing no outliers. (**e**) Scale-free topology analysis for WGCNA soft-threshold selection. The branches represent the samples, and the vertical coordinate represents the height of hierarchical clustering. The horizontal axis represents the value of the weight parameter power, and the vertical axis of the left figure shows the scale-free fit index, namely signed R2. The higher the square of the correlation coefficient, the closer the network is to the scale-free distribution. The vertical axis of the right figure represents the mean value of all gene adjacency functions in the corresponding gene module. (**f**) Module clustering dendrogram. The upper part is the hierarchical clustering tree of genes, and the lower part is the gene module, with different colors representing different modules. (**g**) Module-trait correlation heatmap, highlighting the MEblack module as most associated with MERGs. The darker the color, the higher the correlation. Red is positive correlation and blue is negative correlation.

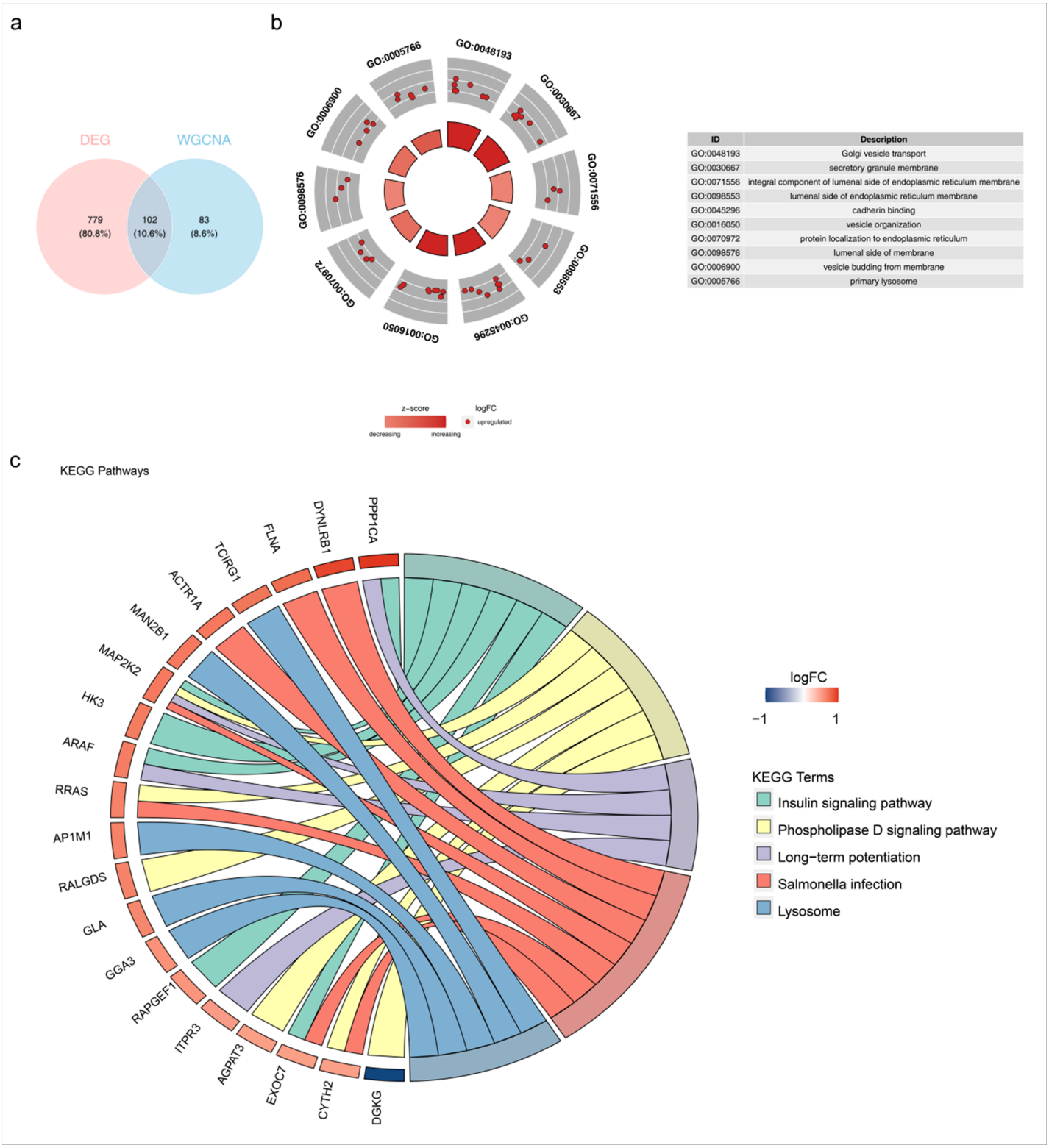


Figure 2

Functional enrichment analysis of candidate genes. (**a**) Venn diagram showing the overlap between CHD-DEGs and ME-related module genes. (**b**) Gene Ontology (GO) enrichment terms for biological processes, cellular components, and molecular functions. The left inner circle shows a bar chart. The height of the bar represents the significance of the Term, with higher values indicating greater significance. The color of the bar indicates the z-score, where darker colors correspond to larger z-

scores. Red and blue bars respectively represent upregulated and downregulated genes. The right side displays descriptions of GO enrichment entries. (**c**) Transcription-quantitative Polymerase Chain Reaction (RT-qPCR) pathway enrichment analysis of candidate genes. On the left is the gene, on the right is the pathway, and the name of the pathway is shown below.

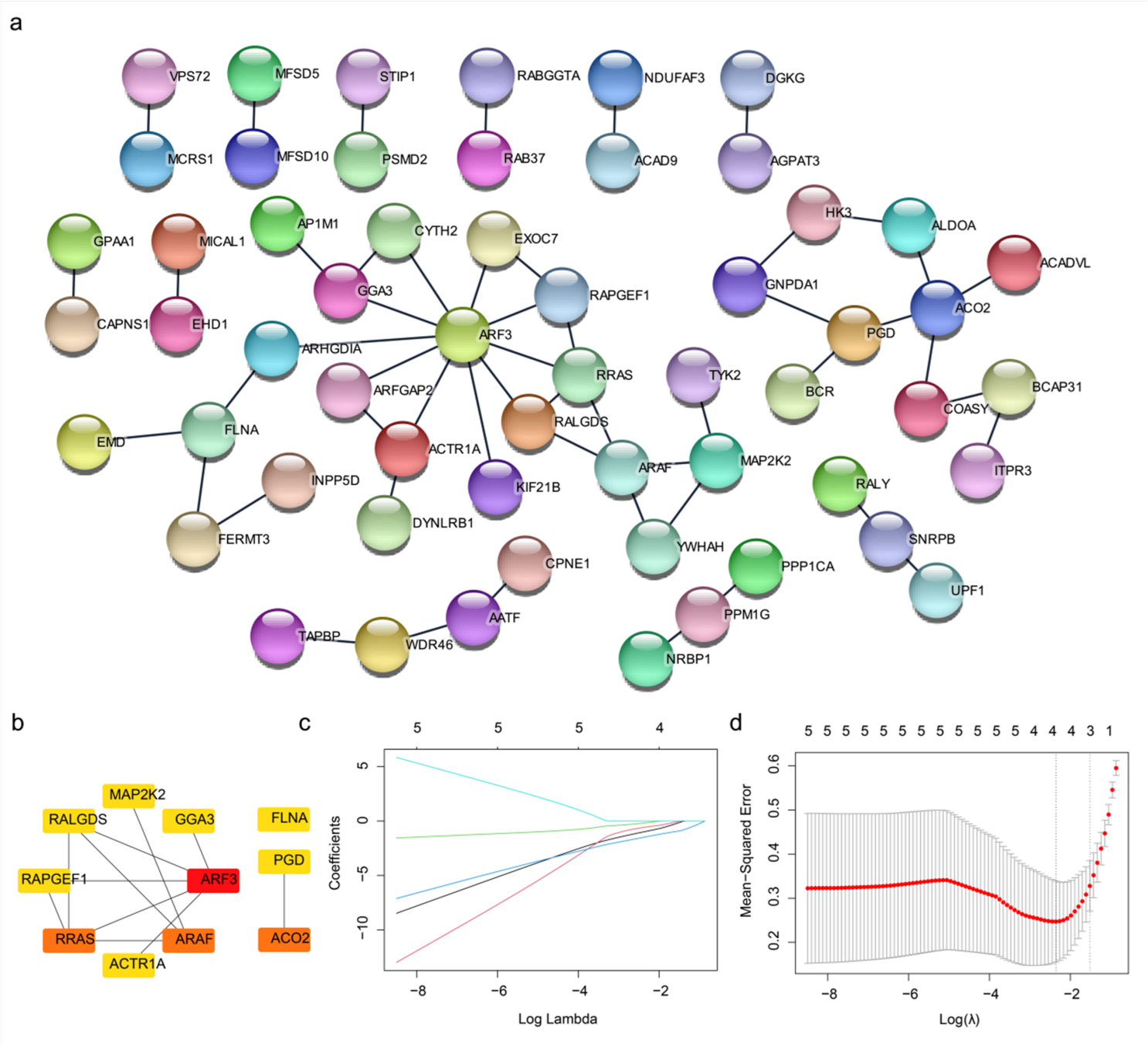


Figure 3

Screening of candidate biomarkers via protein-protein interaction (PPI) network and least absolute shrinkage and selection operator (LASSO) regression. (**a**) PPI network of candidate genes. (**b**) Top hub genes ranked by connectivity scores. (**c**) LASSO coefficient profiles of candidate genes. The horizontal axis is the logarithm of lambdas, and the vertical axis is the coefficient of the variable. Each line

represents a gene. (**d**) Cross-validation curve for optimal lambda selection in LASSO regression. The horizontal axis is the logarithm of lambdas and the vertical axis is the model error.

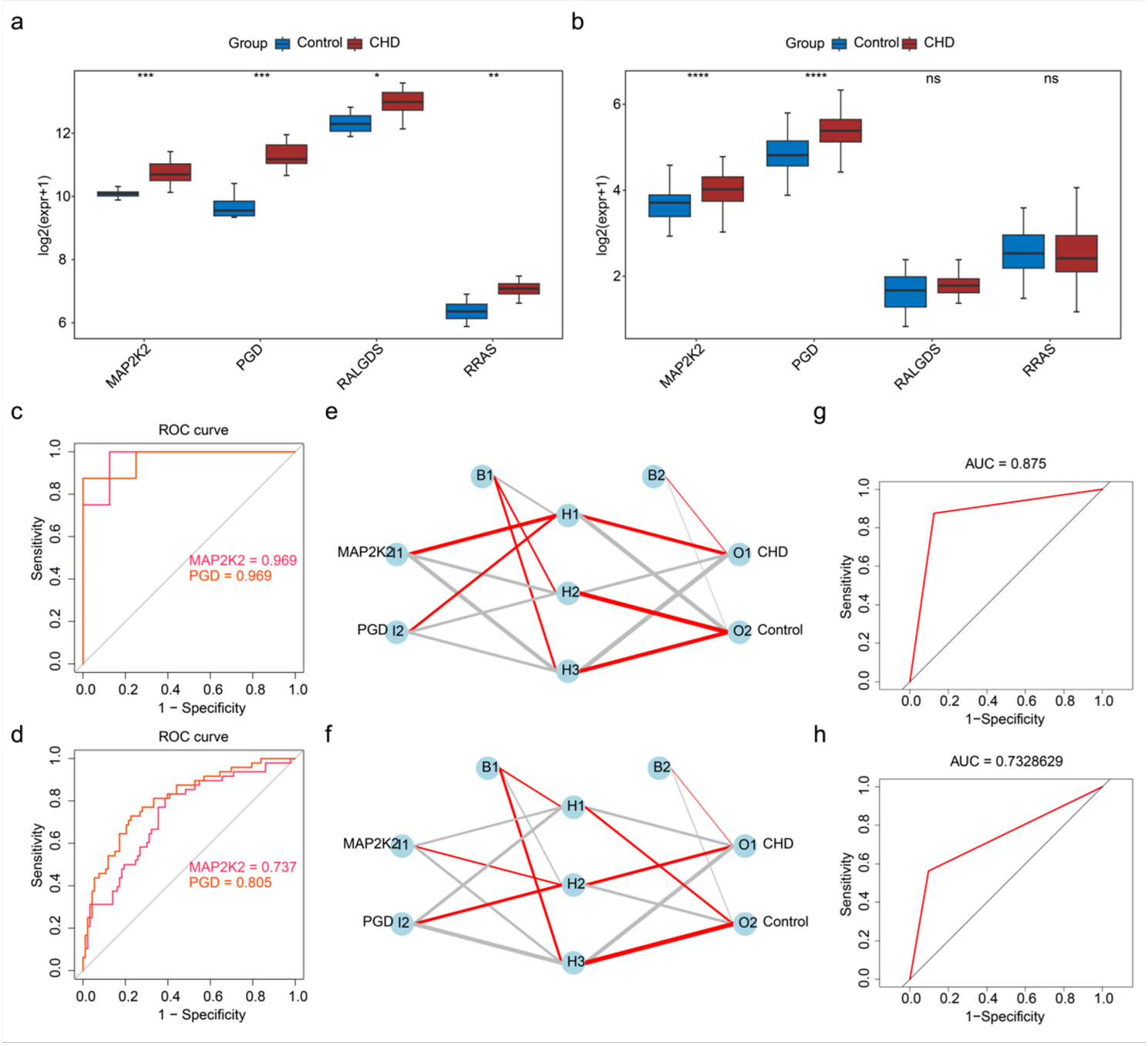


Figure 4

Validation of biomarker diagnostic performance. (**a-b**) Boxplots comparing MAP2K2 and Phosphogluconate Dehydrogenase (PGD) expression levels in Coronary Heart Disease(CHD) vs. control samples across training (GSE179789) and validation (GSE113079) datasets. The horizontal axis is gene; the vertical axis is expression level; red represents disease samples, blue represents control samples; asterisk indicates significance: *, p <0.05; **, p <0.01; ***, p <0.001. (C-D) ROC curves evaluating the diagnostic accuracy of MAP2K2 and PGD in both datasets. (**c**) Training set GSE179789, (D) validation set

GSE113079. (**e-f**)Architecture of the artificial neural network (ANN) model. The nodes marked as "1" in this diagram are called bias units. The leftmost layer (Layer 1) serves as the input layer, the middle layer (Layer 2) is the hidden layer, and the rightmost layer (Layer 3) functions as the output layer. In this configuration, there are 2 input units (including the bias unit), 2 output units, and 3 hidden units (excluding the bias unit). The coefficients in the connections represent weights, which indicate how much each variable contributes to the next node's output. (**g-h**) Artificial neural network ROC curve. The x-axis is specificity and the y-axis is sensitivity. The area enclosed by the curve and the x-axis is called AUC.

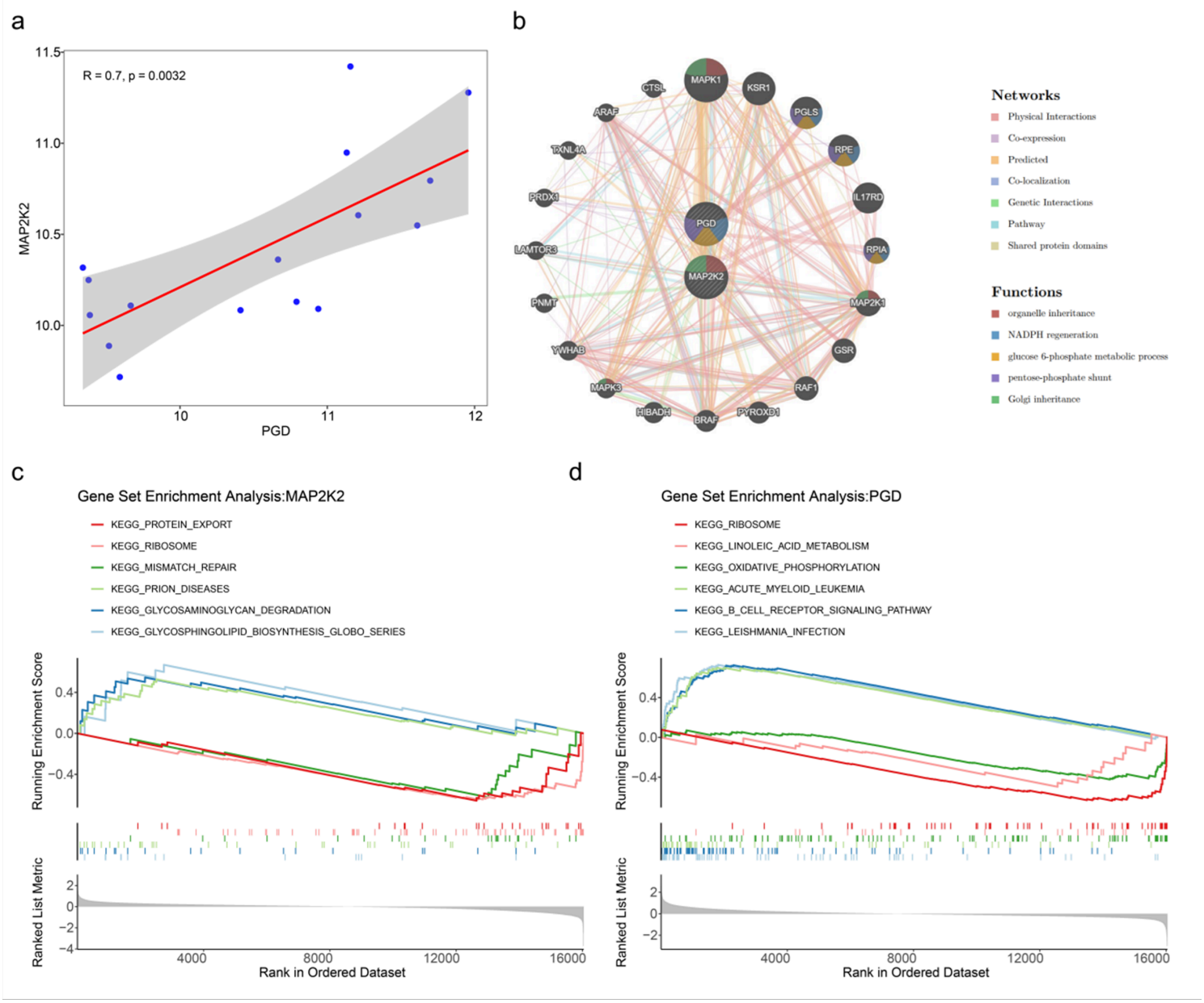


Figure 5

Functional and pathway associations of MAP2K2 and phosphogluconate dehydrogenase (PGD). (**a**) Correlation scatter plot of MAP2K2 and PGD expression levels. The horizontal and vertical coordinates are the expression levels of biomarkers, R represents the correlation, and p represents whether the

correlation is significant. (**b**) Gene-gene interaction (GGI) network of biomarkers and co-expressed genes. (**c-d**) MAP2K2 and PGD GSEA enrichment analysis. The top section displays an enrichment fraction line graph, where each curve represents a pathway. The peak of each curve indicates the pathway's enrichment fraction, with genes preceding the peak being core genes in that pathway. Peaks in the upper-left quadrant represent core genes primarily identified through differential expression analysis based on biological markers' expression levels, while those in the lower-right quadrant indicate core genes mainly identified through differential expression analysis based on high/low marker expression levels. The second section uses dotted lines to mark genes within the gene set. The third section presents the rank value distribution chart for all genes.

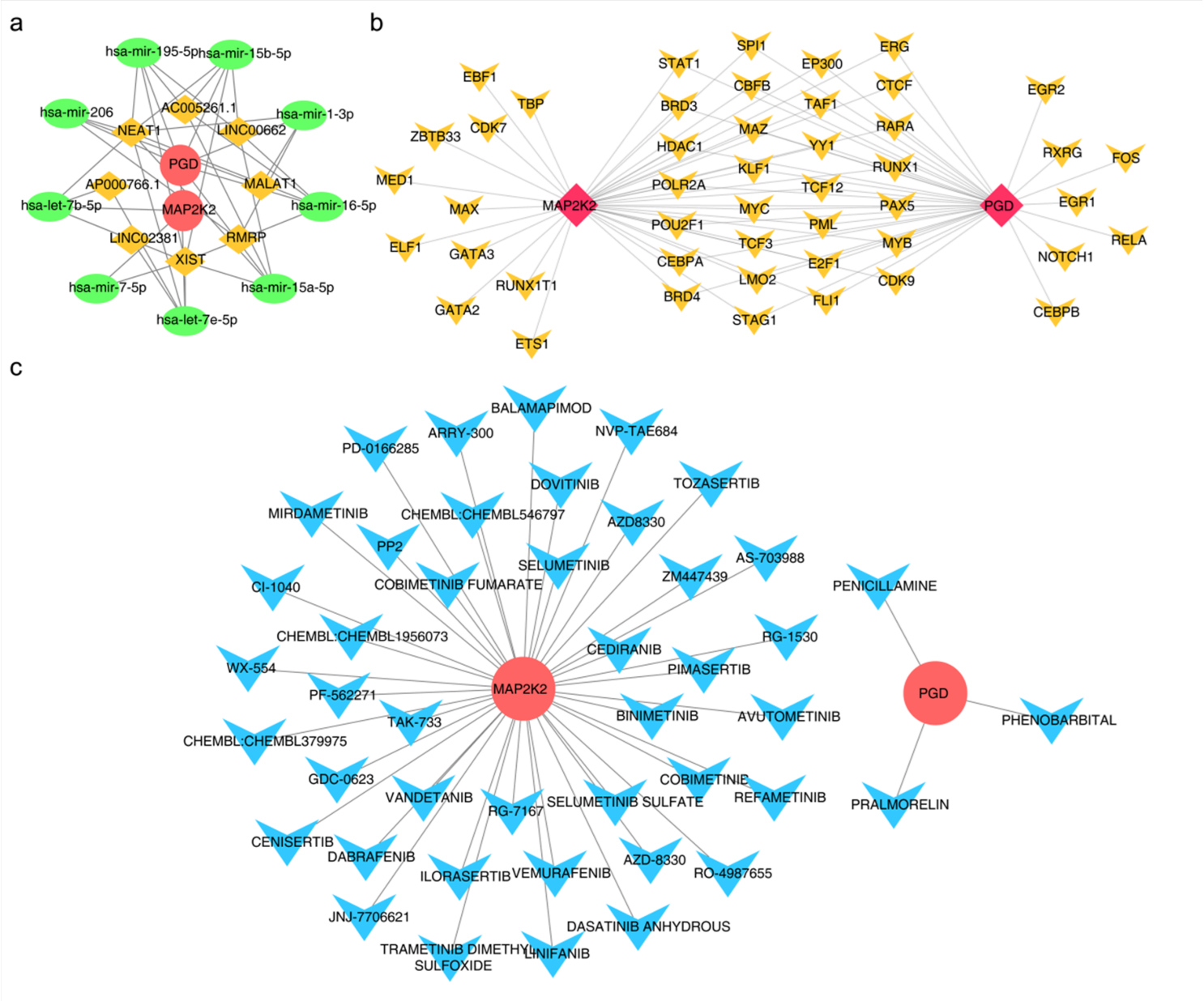


Figure 6

Regulatory networks and drug prediction for biomarkers. (**a**) lncRNA-miRNA-mRNA regulatory network for MAP2K2 and PGD. Red for mRNA; green for miRNA; yellow for lncRNA. (**b**) Transcription factor (TF)-

mRNA interaction network. Red: biomarkers; yellow: transcription factor TF. (**c**) Drug-target network for predicted therapeutic compounds.

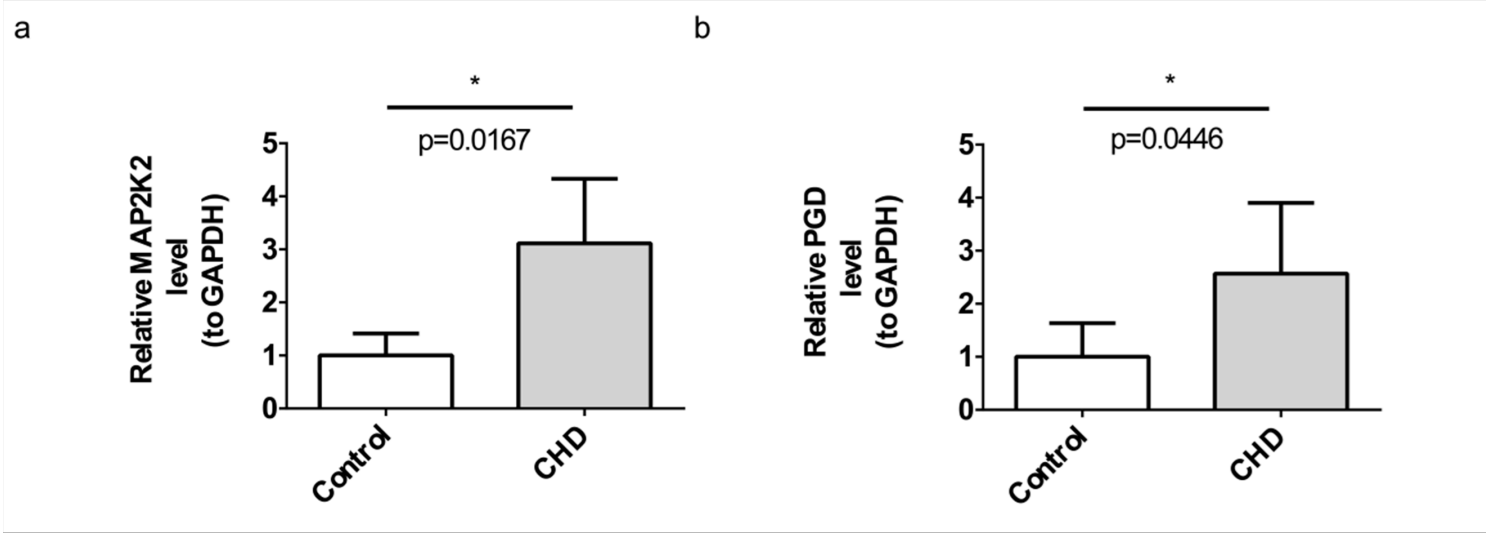


Figure 7

Experimental validation of biomarker expression in clinical samples.(**a-b**) everse Transcription-quantitative Polymerase Chain Reaction (RT-qPCR) results confirming upregulation of MAP2K2 and PGD in CHD tissues compared to controls.

Supplementary Files

This is a list of supplementary files associated with this preprint. Click to download.

- SupplementaryInformation.pdf